Fibroblasts secrete Slit2 to inhibit fibrocyte differentiation and fibrosis

Darrell Pilling[a,1], Zhichao Zheng[a], Varsha Vakil[b], and Richard H. Gomer[a,b,1]

[a]Department of Biology, Texas A&M University, College Station, TX 77843; and [b]Department of Biochemistry and Cell Biology, Rice University, Houston, TX 77251

Edited by Richard Bucala, Yale University School of Medicine, New Haven, CT, and accepted by the Editorial Board November 18, 2014 (received for review September 10, 2014)

Monocytes leave the blood and enter tissues. In healing wounds and fibrotic lesions, some of the monocytes differentiate into fibroblast-like cells called fibrocytes. In healthy tissues, even though monocytes enter the tissue, for unknown reasons, very few monocytes differentiate into fibrocytes. In this report, we show that fibroblasts from healthy human tissues secrete the neuronal guidance protein Slit2 and that Slit2 inhibits human fibrocyte differentiation. In mice, injections of Slit2 inhibit bleomycin-induced lung fibrosis. In lung tissue from pulmonary fibrosis patients with relatively normal lung function, Slit2 has a widespread distribution whereas, in patients with advanced disease, there is less Slit2 in the fibrotic lesions. These data may explain why fibrocytes are rarely observed in healthy tissues, may suggest that the relative levels of Slit2 present in healthy tissue and at sites of fibrosis may have a significant effect on the decision of monocytes to differentiate into fibrocytes, and may indicate that modulating Slit2 signaling may be useful as a therapeutic for fibrosis.

fibrocyte | lung | fibrosis | Slit2 | fibroblast

To help form granulation tissue during wound healing, monocytes leave the circulation, enter the tissue, and differentiate into fibroblast-like cells called fibrocytes (1–4). Fibrocytes are also found in lesions associated with fibrotic diseases such as pulmonary fibrosis, congestive heart failure, cirrhosis of the liver, and nephrogenic systemic fibrosis (3, 5–9). Fibrocytes express markers of both hematopoietic cells (CD34, CD45, FcγR, LSP-1, and MHC class II) and stromal cells (collagens, fibronectin, and matrix metalloproteases) (2, 3, 10–12). Fibrocytes also promote angiogenesis by secreting VEGF, bFGF, IL-8, and PDGF and promote fibroblast proliferation, migration, and collagen production by secreting TGF-β and CTGF (13, 14). Fibrocyte recruitment and differentiation is regulated by a variety of factors (3, 15). In vitro, monocytes can differentiate into fibrocytes without the addition of any exogenous factors (5, 11, 12, 16–22). A key question about fibrocyte differentiation and fibrosis is why, in healthy tissues where monocytes and macrophages are readily identified, fibrocytes are rarely observed (3, 8, 23–26).

In tissues, fibroblasts are a major cell population and can modulate the immune system (27–30). In this report, we show that fibroblasts secrete the neuronal guidance protein Slit2 and that Slit2 inhibits fibrocyte differentiation. In addition, we show that injections of Slit2 reduce bleomycin-induced pulmonary fibrosis in mice. Finally, we show that, in the mouse pulmonary fibrosis model as well as human patients with pulmonary fibrosis, there seems to be a decrease in Slit2 levels in the lungs, suggesting that pulmonary fibrosis may be in part a Slit2 deficiency disease. These data suggest that the relative level of Slit2 present at sites of wound healing, inflammation, and fibrosis may have a profound effect on the ability of monocytes to differentiate into fibrocytes.

Results

Fibroblasts Inhibit Human Fibrocyte Differentiation. By secreting collagen and fibronectin, fibrocytes can effectively replace a fibroblast (3). In a healthy tissue, there is a sufficient local density of fibroblasts so no additional fibroblasts (or fibrocytes) would be needed. To test the hypothesis that fibroblasts might secrete soluble factors to signal monocytes that have entered the tissue to not differentiate into fibrocytes, we added conditioned medium from human fibroblasts (FCM) to human peripheral blood mononuclear cells (PBMCs) in conditions where some of the monocytes in the PBMCs would normally differentiate into fibrocytes. The PBMCs were cultured for 5 d in serum-free medium (SFM) with FCM from human adult skin, adult lung, and MRC5 fetal lung fibroblasts. In the absence of fibroblast conditioned medium, we observed 520–1,660 fibrocytes per 10^5 PBMCs from the different donors, similar to what we and others have previously observed (10, 11, 18, 31). Because of this variability, for each donor, fibrocyte numbers were normalized to serum-free controls. For all donors, compared with the control with no added FCM, 10% and above FCM significantly inhibited fibrocyte differentiation (Fig. 1 *A*–*C*).

To verify that the FCM was affecting the number of fibrocytes and to determine whether FCM altered the phenotype of fibrocytes, we stained PBMCs after 5 d of culture with or without FCM for fibrocyte markers (Fig. 1 *D*–*K*). In the absence of FCM, the elongated cells were positive for markers expressed by fibrocytes, including CD13 and CD45, and had no observable staining for the macrophage marker CD163. In the presence of 30% FCM, the number of fibrocytes was significantly reduced although macrophages were readily detected, as determined by the expression of CD13, CD14, and CD163.

Fibroblasts Secrete Slit2, Which Inhibits Fibrocyte Differentiation. The factor (or factors) secreted by the fibroblasts were stable when stored for 2 wk at 4 °C or frozen at −20 °C or −80 °C. We tested the FCM for cytokines known to regulate fibrocyte

Significance

A key question in fibrosing diseases is why monocytes do not become fibrocytes in healthy tissues but can become fibrocytes in fibrotic lesions. We show that fibroblasts secrete a signal that inhibits the differentiation of monocytes into fibrocytes. We identify the signal as Slit2 and show that Slit2 levels are low in fibrotic lesions. We also show that injection of Slit2 prevents fibrosis in a mouse model of lung fibrosis. The identification of Slit2 as a key signal in normal tissues that prevents entering monocytes from becoming fibrocytes represents a major advance in our understanding of the regulation of the innate immune system and how fibrosis propagates, as well as a potential novel therapeutic for fibrosis.

Author contributions: D.P. and R.H.G. designed research; D.P., Z.Z., and V.V. performed research; D.P., Z.Z., V.V., and R.H.G. analyzed data; and D.P. and R.H.G. wrote the paper.

The authors declare no conflict of interest.

This article is a PNAS Direct Submission. R.B. is a guest editor invited by the Editorial Board.

[1]To whom correspondence may be addressed. Email: rgomer@tamu.edu or dpilling@bio.tamu.edu.

This article contains supporting information online at www.pnas.org/lookup/suppl/doi:10.1073/pnas.1417426112/-/DCSupplemental.

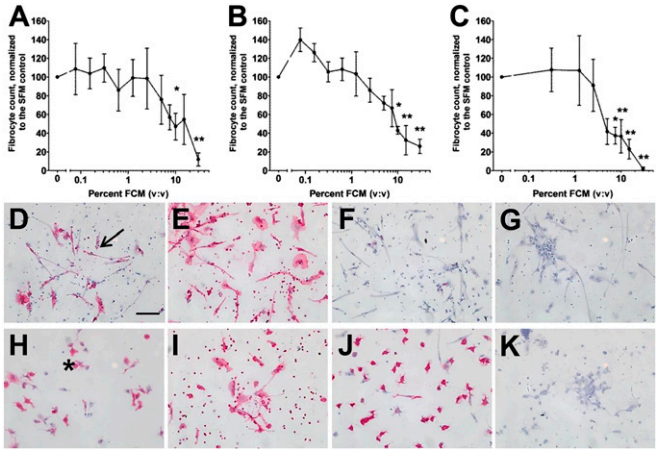

Fig. 1. Fibroblast-secreted factors inhibit fibrocyte differentiation. Human normal adult (*A*) lung, (*B*) dermal, and (*C*) MRC-5 fetal lung fibroblast conditioned medium (FCM) was collected, and human peripheral blood mononuclear cells (PBMCs) were cultured in the presence or absence of FCM for 5 d. Values are mean ± SEM ($n = 5$). *$P < 0.05$ and **$P < 0.01$ compared with the no-FCM control (*t* test). (*D*–*K*) PBMCs were cultured for 5 d in (*D*–*G*) SFM or (*H*–*K*) 30% MRC-5 FCM. After 5 d, PBMCs were air-dried, fixed, and stained with antibodies against (*D* and *H*) the fibrocyte and macrophage marker CD13, (*E* and *I*) the pan leukocyte marker CD45, (*F* and *J*) the macrophage marker CD163, and (*G* and *K*) mouse IgG1 antibodies (red staining). Cells were then counterstained with hematoxylin to identify nuclei (blue). Photomicrographs are representative results from five different donors. The spindle-shaped elongated cells are fibrocytes. Arrow points to a fibrocyte, and * indicates a cluster of macrophages. (Scale bar: 100 μm.)

differentiation or involvement in fibrotic responses. We did not detect any cytokines known to regulate fibrocyte differentiation, such as IL-4, IL-10, IL-12, IL-13, or IFN-γ (Fig. S1*A*). We did detect IL-6, along with low levels of TNF-α, but we have previously shown that these cytokines do not significantly affect fibrocyte differentiation (17). To determine if the factor secreted by fibroblasts was secreted by other cells, we cultured PBMCs in the presence of 30% (vol/vol) conditioned medium from HEK293 cells, which secrete a wide variety of proteins (32, 33). Compared with cells cultured in SFM, we found that MRC5-FCM inhibited fibrocyte differentiation, but HEK293-CM did not (Fig. S1*B*). Fractionation with centrifugal filters indicated that the inhibitory activity secreted by fibroblasts was a factor larger than 100 kDa (Fig. 2*A*). We then fractionated the FCM by ion exchange chromatography (Fig. 2*B*). The inhibitory factor(s) eluted from an anion exchange column as a single peak in fractions 24 (fibrocyte counts 31% of control) and 25 (42.5% of control) whereas the adjacent fractions 20–23 and 26–31 had fibrocyte counts ~98% of control. Using mass spectrometry of tryptic digests, we identified several components of the active peak (Table S1). Of these proteins, only albumin and the neuronal repellent factor Slit2 are known to be extracellular proteins (34). We previously observed that albumin does not inhibit fibrocyte differentiation (18), suggesting that a possible candidate for the inhibitory factor in FCM is Slit2.

Recombinant murine Slit2 (rSlit2) protein (97% identity with human Slit2), corresponding to a 100-kDa portion (Gln26 to Gln900) of the N-terminal domain of Slit2, inhibited human (Fig. 3*A*) and murine (Fig. S2) fibrocyte differentiation. The rSlit2 IC_{50} for inhibiting human fibrocyte differentiation was 0.33 ± 0.13 ng/mL, with a Hill coefficient of 0.305 ± 0.08 (mean ± SEM, $n = 3$). To determine whether the inhibition of fibrocyte differentiation by Slit2 is a direct effect on monocytes, or due to an indirect effect on the B cells, dendritic cells, NK cells, or T cells, present within the PBMC preparation, we incubated isolated human monocytes with rSlit2 (Fig. 3*A*). For all donors, rSlit2 significantly inhibited fibrocyte differentiation from isolated monocytes, with an IC_{50} of 0.56 ± 0.13 ng/mL and a Hill coefficient of 0.41 ± 0.06 (mean ± SEM, $n = 3$). The IC_{50} and Hill coefficient for monocytes was not significantly different from those of PBMCs (*t* tests). These data suggest that Slit2 acts directly on monocytes to inhibit fibrocyte differentiation.

Slit2 binds to the Robo1 receptor on monocytes, macrophages, neutrophils, and dendritic cells (35–37). We observed that Robo1 is expressed on fibrocytes and macrophages and that incubating PBMCs with Slit2 led to reduced fibrocytes, but no obvious changes in Robo1 levels on macrophages (Fig. S3).

To determine if removal of Slit2 from FCM would alter the ability of FCM to decrease fibrocyte differentiation, Slit2 was depleted from FCM using protein G beads coated with anti-Slit2 antibodies. Compared with untreated FCM, removal of Slit2 from MRC5 FCM (Fig. 3*B*) or dermal FCM (Fig. S4) led to a significant reduction in the ability of FCM to inhibit human fibrocyte differentiation. The uncoated beads, and beads coated with either rabbit IgG or rabbit antibodies against HSP47, did not significantly alter the inhibition of fibrocyte differentiation by FCM (Fig. 3*B* and Fig. S4). These data suggest that Slit2 is the active factor in FCM that inhibits fibrocyte differentiation.

In the Bleomycin Model, the Early Stages of Inflammation Are Associated with a Deficiency of Slit2. Bleomycin aspiration leads to epithelial cell damage, inflammation, collagen deposition, and fibrosis, and these changes also reduce lung function and peripheral blood oxygen content (38, 39). BAL fluid from mice at day 3 was collected to determine if in the early stages of bleomycin-induced inflammation, there were altered levels of Slit2 protein. In vivo, Slit2 is normally found as a combination of the full-length protein and several cleavage products (Fig. S5) (40). In untreated (control) mice, three major isoforms of Slit2 could be identified (Fig. 4*A*). In mice that had aspirated saline alone (NaCl; the buffer solution for the bleomycin), the three isoforms were also readily detected. However, in the BAL of mice treated with bleomycin, there was a reduction in the amount of all three isoforms of Slit2 (Fig. 4*A*). These data indicate that, in the murine bleomycin model of pulmonary fibrosis, the initial stage is accompanied by a deficiency of endogenous Slit2.

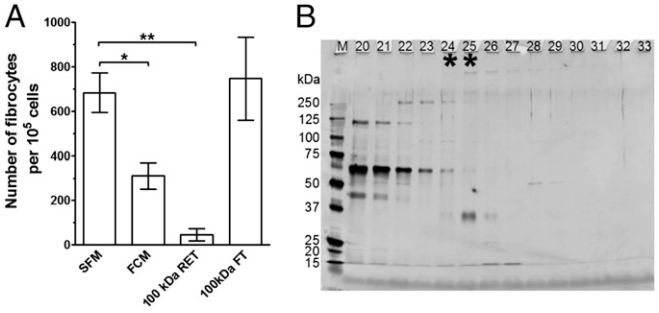

Fig. 2. Fractionation of FCM and identification of Slit2. (*A*) FCM was fractionated by centrifugation using 100-kDa filters. PBMCs were cultured for 5 d in the presence or absence of 10% (vol/vol) FCM, 10-fold concentrated 100-kDa retentate (Ret), or 100-kDa flow through (FT). After a 5-d incubation, cells were air-dried, fixed, and stained, and the number of fibrocytes was counted. Compared with PBMCs cultured in the absence of conditioned medium (SFM), FCM and the 100-kDa retentate significantly decreased the number of fibrocytes. Values are mean ± SEM ($n = 4$). *$P <$ 0.05 and **$P < 0.01$ (1-way ANOVA, Tukey's test). (*B*) Fractions from ion exchange chromatography of the 100-kDa retentate were analyzed by PAGE on a 10% reducing gel. M, molecular mass markers with masses in kDa are indicated at left. The * indicates fractions containing inhibitory activity. The gel is representative of three independent experiments.

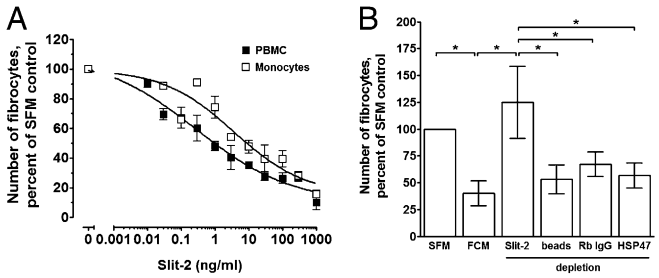

Fig. 3. The effect of recombinant Slit2 (rSlit2) on human fibrocyte differentiation. (*A*) Human PBMCs and isolated monocytes were cultured in the presence or absence of rSlit2 for 5 d. Cells were then air-dried, fixed, and stained, and fibrocytes were counted. Values are mean ± SEM ($n = 3$). The absence of error bars indicates that the error was smaller than the plot symbol. rSlit2 concentrations at 0.1 ng/mL and above significantly inhibited fibrocyte differentiation (*t* test). Lines are fits to sigmoidal dose–response curves with variable Hill coefficients. (*B*) MRC-5 FCM was incubated with beads labeled with anti-Slit2 antibodies, anti-HSP-47 (a control protein depletion), rabbit IgG (a control IgG), or unlabeled beads. Human PBMCs were cultured in the presence or absence of 10% (vol/vol) antibody-depleted FCM for 5 d. Values are mean ± SEM ($n = 4$). $^*P < 0.05$ (1-way ANOVA, Tukey's test).

Slit2 Injections Reduce Bleomycin-Induced Lung Inflammation. Because fibrocytes participate in fibrosis and Slit2 inhibits fibrocyte differentiation, we tested the hypothesis that Slit2 might inhibit fibrosis. After bleomycin aspiration, C57BL/6 mice were treated with daily i.p. injections of rSlit2 or buffer from day 1–14. To determine if rSlit2 injections altered the response to bleomycin aspiration, we measured arterial oxygen saturation (pulse Ox). At 21 d after bleomycin aspiration, compared with mice that received saline injections, mice that received rSlit2 injections had no significant reduction in pulse Ox compared with control mice (Fig. 4*B*). Mice were then euthanized. The weakly adhered cells from the airways were collected by bronchoalveolar lavage (BAL), and total BAL cells were counted (Fig. 4*C*). The BAL cells were also stained for CD11b to identify newly recruited inflammatory macrophages and neutrophils (Fig. 4*D*), and CD11c to identify alveolar macrophages and dendritic cells (Fig. S6*B*). As previously observed (38, 39, 41, 42), bleomycin increased the total number of cells (Fig. 4*C*), the number of macrophages and lymphocytes as assessed by morphology (Fig. S6*A*), and the percentage of CD11b-positive cells in the BAL (Fig. 4*D*). Compared with mice treated with bleomycin and then given PBS injections, mice treated with bleomycin and then given rSlit2 injections had decreased total number of macrophages, lymphocytes, and percentage of CD11b-positive cells in the BAL. We also observed that the reduction in the percentage of CD11c-positive cells in the BAL after bleomycin was reversed by Slit2 injections (Fig. S6*B*).

After BAL, lungs were sectioned and stained with CD45 to detect interstitial inflammation (Fig. 5 *A–D*). Bleomycin instillation caused a disruption of the normal lung architecture, along with areas of inflammatory cell infiltrates (Fig. 5*C*), and this inflammation was reduced by rSlit2 injections (Fig. 5*D*). Lung sections were also stained to detect other cells that were not removed by BAL. As previously observed (38, 39, 41, 42), bleomycin increased the number of $CD11b^+$, $CD11c^+$, and $CD45^+$ cells in the lungs (Fig. 5*E*). For mice treated with bleomycin, compared with PBS injections, rSlit2 injections significantly reduced the number of $CD11b^+$, $CD11c^+$, and $CD45^+$ cells in the lungs (Fig. 5*E*). At 21 d, the presence or absence of bleomycin, or the presence or absence of rSlit2 injections, did not significantly alter the numbers of CD3-positive T cells, CD209b (Sign-R1)-positive dendritic cells, or Ly6G-positive neutrophils (Fig. 5*E*). Together, these data indicate that injections of rSlit2 can reduce lung inflammation after bleomycin aspiration.

Slit2 Injections Reduce Bleomycin-Induced Lung Fibrosis. To determine if rSlit2 injections also reduced the bleomycin-induced fibrotic response, lung sections were stained for collagen-I or collagen-VI, or stained with picrosirius red to detect collagen. As previously observed (23, 38, 39), lung collagen levels were increased at 21 d after bleomycin treatment compared with saline controls (Fig. 6*A* and Fig. S7). For mice treated with bleomycin, compared with injections of PBS, injections of rSlit2 significantly decreased the amount of collagen in the lungs (Fig. 6*A* and Fig. S7). Lung sections were also stained for fibrocytes. As previously observed (5, 23, 43), bleomycin increased the number of fibrocytes in the lungs (Fig. 6*B*). For mice treated with bleomycin, compared with PBS injections, rSlit2 injections significantly reduced the number of fibrocytes in the lungs (Fig. 6*B*). These data suggest that, in the murine bleomycin model of pulmonary fibrosis, Slit2 injections can reduce fibrosis.

Slit2 Is Expressed by Lung Fibroblasts and Epithelial Cells. Slit2 is present in the murine fetal lung and also expressed by club cells (Clara cells) in the adult mouse (44, 45). However, little is known about the expression of Slit2 by other cells present in human lung. We observed that human lung fibroblasts and bronchial epithelial cells produce Slit2 (Fig. S8). These data indicate that the local production of Slit2 by fibroblasts and epithelial cells may prevent the differentiation of monocytes into fibrocytes in normal lung tissue.

Slit2 Levels May Be Abnormally Low in Pulmonary Fibrosis Lesions. To determine if Slit2 is associated with human lung fibrosis, we examined the distribution of Slit2 in lung tissue from chronic obstructive pulmonary disease (COPD) patients with relatively normal lungs [>80% forced vital capacity (FVC)] and pulmonary fibrosis patients with advanced disease (<50% FVC) (Table S2). Lung tissue from patients with an FVC of >80% showed a widespread

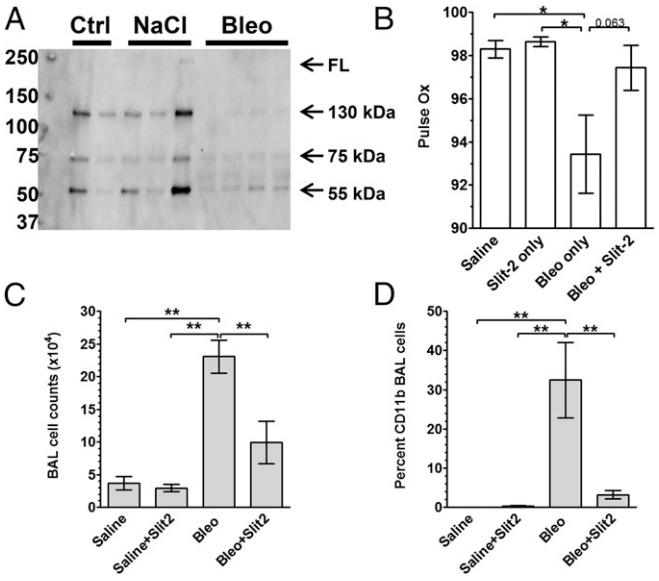

Fig. 4. Changes in Slit2 protein, pulse Ox, and BAL cell number after bleomycin aspiration. (*A*) BAL from mice was analyzed by Western blotting using an antibody to the C-terminal portion of Slit2. This antibody detects the full-length (FL) protein and the 55-, 75-, and 130-kDa fragments. $n = 2$ naive (Ctrl) mice, $n = 3$ saline aspiration (NaCl), $n = 4$ bleomycin aspiration (Bleo). (*B*) Mice were assessed for peripheral blood oxygen content (pulse Ox). (*C*) The total number of cells collected from the BAL at day 21. (*D*) The percentage of $CD11b^+$ inflammatory cells in the BAL at day 21. (*B–D*) Values are mean ± SEM ($n = 3$–4 mice per group). $^*P < 0.05$, $^{**}P < 0.01$ (1-way ANOVA, Tukey's test).

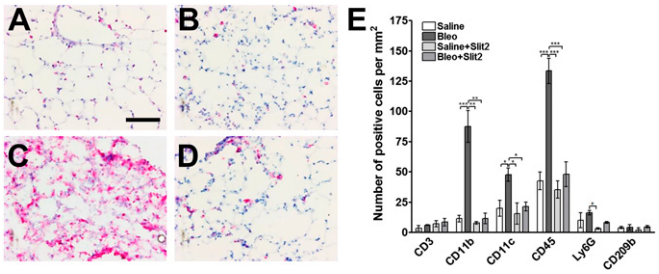

Fig. 5. Changes in lung tissue leukocyte populations after bleomycin instillation. Day 21 lungs were stained with antibodies against CD45 to show cellular inflammation. (*A*) Lung section after saline aspiration and PBS injections. (*B*) Lung section after saline aspiration and Slit2 injections. (*C*) Lung section after bleomycin aspiration and PBS injections. (*D*) Lung section after bleomycin aspiration and Slit2 injections. (Scale bar: 0.1 mm.) (*E*) Cryosections of mouse lungs were stained with antibodies against CD3 (T cells), CD11b (neutrophils and inflammatory macrophages), CD11c (resident macrophages and dendritic cells), CD45 (total leukocytes), Ly6G (neutrophils), and CD209b (Sign-R1 dendritic cells). Values are mean ± SEM (n = 3–4 mice per group). *$P < 0.05$, **$P < 0.01$, ***$P < 0.001$ (1-way ANOVA, Tukey's test).

distribution of Slit2 (Fig. 7). In lung tissue from pulmonary fibrosis patients with advanced disease, Slit2 distribution was significantly reduced (Fig. 7*H*). These data suggest that human pulmonary fibrosis may involve a deficiency in Slit2.

Discussion

We found that fibroblast-derived Slit2 inhibits fibrocyte differentiation. In addition, rSlit2 injections inhibit bleomycin-induced murine lung fibrosis. In human fibrotic lung tissue, we found that the distribution of Slit2 was widespread, but Slit2 had a restricted distribution and was apparently absent from the fibrotic areas. These data suggest that the relative levels of Slit2 present in normal tissue and at sites of fibrosis may have a significant effect on the ability of monocytes to differentiate into fibrocytes.

Slit proteins bind a series of receptors called Robo, with mammals having four receptors, Robo1 to -4 (46, 47). Immune cells, including monocytes, macrophages, and monocyte-derived dendritic cells, express Robo receptors (35, 36, 48). In the nervous system, Slit–Robo interactions inhibit the migration of neuronal cells and prevent axons from recrossing the ventral midline during development of the CNS (40, 49). Knockouts of Slit2 and its major receptor Robo1 are embryonic lethal, with defects in neuronal and lung development (50, 51). Slit2 also inhibits the migration of neutrophils, dendritic cells, T cells, and macrophages both in vitro and in vivo (35–37, 45, 52–54). However, Slit2 promotes eosinophil migration (45), and Slit3 and, to a lesser extent, Slit1 promote monocyte migration (48). Our results showing that Slit2 inhibits monocyte to fibrocyte differentiation suggest an additional function for Slit2 in the innate immune system. In addition, the Slit2 injections may also regulate the migration of monocytes and/or fibrocyte precursors entering the lung after bleomycin challenge (3, 55, 56). However, because the Slit2 injections were systemic, rather than inhaled, this treatment would not generate a local gradient of Slit2, but rather inhibit generalized migration. Further work investigating the local application of Slit2 in the lung is required to determine the mechanism of action.

Slit2 is present in murine fetal lung and adult rat lung and is expressed by club cells in the adult mouse (44, 45, 52). However, little is known about the expression of Slit2 in human lung tissue during inflammation and fibrosis. Loss of Slit2 mRNA has been shown to correlate with antibody-induced glomerulonephritis in the rat (53). The observation that Slit2 is produced by fibroblasts and epithelial cells suggests that these cells may be an additional source of antifibrotic molecules in normal lung tissue. In addition, the loss of Slit2 production may augment profibrotic signals present in tissues after a fibrotic insult. Whether the reduced levels of Slit2 seen in human fibrotic tissue is due to a loss of Slit2-producing cells, such as club cells, or the presence of factors that down-regulate Slit2 production is unclear. However, the consequences of one or both mechanisms will lead to reduced Slit2 levels and the generation of a profibrotic environment. Together, our results suggest that Slit2 levels are important in the regulation of lung inflammation and fibrosis and that therapeutic use of Slit2 may be beneficial in regulating fibrosis.

Materials and Methods

Cell Isolation. Human peripheral blood was collected from healthy adult volunteers who gave written consent and with specific approval from the Texas A&M University human subjects Institutional Review Board. Peripheral blood mononuclear cells (PBMCs) were isolated from blood using Ficoll-Paque Plus (GE Healthcare Biosciences), as described previously (18). Monocytes were enriched from PBMCs using EasySep monocyte enrichment kits (StemCell Technologies), as described previously (57). Spleen cells from 4- to 6-wk-old male C57BL/6J mice (The Jackson Laboratory) were isolated as described previously (19).

Fibroblasts. Human MRC5 fibroblasts (ATCC) and primary human dermal and lung fibroblasts (Lonza) were grown in RPMI-1640 (Sigma-Aldrich), as described previously (27). To make fibroblast conditioned medium (FCM), ~80% confluent fibroblast cultures in 75-cm^2 flasks (BD Bioscience) were rinsed three times with FibroLife basal medium (LifeLine Cell Technology) and then incubated in FibroLife basal medium for 2–3 h to remove exogenous serum products. The basal medium was removed, the cells were rinsed three times with basal medium, and fibroblasts were then cultured in FibroLife protein-free medium (PFM), containing FibroLife basal medium supplemented with 10 mM Hepes, 1× nonessential amino acids, 1 mM sodium pyruvate, 100 U/mL penicillin, 100 μg/mL streptomycin (all from Sigma-Aldrich), and 2 mM glutamine (Invitrogen). After 3 d, the medium was collected, clarified by centrifugation at 500 × g for 10 min, and stored at 4 °C. Clarified conditioned medium was used within 2 d. Conditioned media were analyzed for cytokines using an ELISArray kit (SABiosciences). HEK293 cells (Life Technologies) and human lung bronchial epithelial cells (PromoCell) were cultured following the vendor's protocol.

Purification and Characterization of Slit2. FCM was fractionated using 100-kDa cutoff centrifugal filters (Amicon Ultra; Millipore) as described previously (23). Chromatography was performed using an AKTA system (GE Healthcare Bio-Sciences). Then, 100 mL of FCM was concentrated with a 100-kDa cutoff centrifugal filter (Amicon) and then washed three times with 10 mL of 10 mM sodium phosphate buffer, pH 7.4 (SB). The retained material was resuspended in 1 mL of SB and loaded onto a 1-mL anion exchange column (HiTrap Q; GE Healthcare), and the column was washed extensively in 10 mM sodium phosphate buffer, pH 7.4, until the absorbance at 280 nm returned to baseline. Bound material was eluted using 50 mL of SB, with a 0- to 1,000-mM gradient of NaCl. The fractions that inhibited fibrocyte differentiation

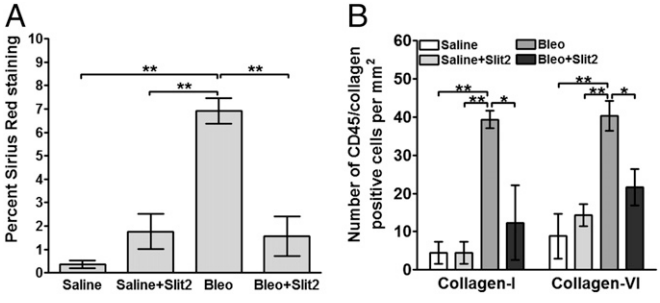

Fig. 6. Changes in lung fibrosis after bleomycin instillation. (*A*) Day-21 lungs were stained with picrosirius red to show collagen deposition. The percentage area stained with picrosirius red was quantified as a percentage of the total area of the lung. (*B*) Lung sections were stained with CD45 and collagen antibodies, and the number of dual positive fibrocytes was counted. Values are mean ± SEM (n = 3–4 mice per group). *$P < 0.05$, **$P < 0.01$ (1-way ANOVA, Tukey's test).

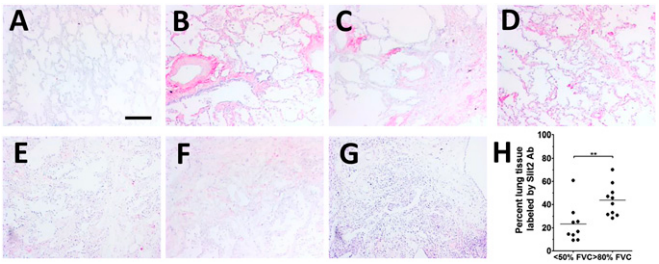

Fig. 7. Reduced Slit2 in pulmonary fibrosis patients with advanced disease. Lung-tissue sections from pulmonary fibrosis patients were stained with anti–N-terminal Slit2 antibodies. (*A–D*) Lung sections from idiopathic pulmonary fibrosis (IPF) patients with FVC >80%. (*E–G*) Lung sections from patients with IPF FVC <50%. (*A*) Lung sections stained with control rabbit antibodies. (*B–D* and *E–G*) Lung sections stained with anti-Slit2 antibodies. (Scale bar: 0.2 mm.) (*H*) The percentage area stained with Slit2 antibodies was quantified as a percentage of the total area of the lung. Values are for individual patient samples, with the sample mean indicated with a bar (n = 9–10 patients per group). $^{**}P < 0.01$ (t test).

were pooled, concentrated, and desalted using 100-kDa cutoff centrifugal filters and SB, as described previously (23). Fractions that inhibited fibrocyte differentiation were digested with trypsin and analyzed at the Mass Spectrometry and Proteomics Core Facility, University of Utah, Salt Lake City.

Immunodepletion of Slit2 was performed as described previously (11). Briefly, 0.5 mL of FCM was incubated overnight at 4 °C with a 0.1-mL packed volume of protein G magnetic beads (Life Technologies), coated with 100 μg of rabbit anti-Slit2 antibodies (Epitomics/Abcam), rabbit anti-HSP-47 (Epitomics/Abcam) as a control, rabbit IgG (Jackson ImmunoResearch) as a control, or unlabeled beads. Beads were then removed by magnetic separation, and the immunodepleted FCM was added to cells.

Fibrocyte Differentiation Assays. Human and murine cells were cultured in FibroLife SFM, as described previously (18), in the presence or absence of FCM or recombinant murine Slit2 (R&D Systems). After 5 d, plates were air-dried, fixed, and stained, and fibrocytes were identified as described previously (11, 18).

Bleomycin-Induced Lung Inflammation. This study was carried out in accordance with the recommendations in the *Guide for the Care and Use of Laboratory Animals* (58) of the National Institutes of Health. The protocol was approved by the Texas A&M University Animal Use and Care Committee. All procedures were performed under anesthesia, and all efforts were made to minimize suffering. To induce fibrosis, 4- to 6-wk-old C57BL/6 mice (The Jackson Laboratory) were treated with an oropharyngeal aspiration of 50 μL of 3 U/kg bleomycin (EMD Millipore) in 0.9% saline or saline alone, as described previously (39, 41, 42, 59). Starting 24 h after bleomycin aspiration, mice were given daily i.p. injections of 2 μg of recombinant mouse Slit2 (R&D Systems) in 0.05 mL of PBS, or PBS alone, from day 1–14 after bleomycin aspiration (13 d total). Mice were euthanized 21 d after bleomycin aspiration, and bronchoalveolar lavage (BAL) cells were collected and counted, and cytospins were prepared as described previously (39, 41, 42, 60). After BAL, lungs were inflated with and embedded in optimal cutting temperature (OCT) compound (VWR), frozen, and stored as described previously (23, 39).

Immunohistochemistry and Western Blotting. PBMCs, fibroblasts, or lung epithelial cells, were cultured for 5 d on eight-well glass microscope slides (Millipore) and then fixed and stained as described previously (12). The PBMCs were stained with mouse monoclonal antibodies to CD13 (clone WM15; BD Biosciences) to detect monocyte-derived cells and fibroblasts, CD45 (clone HI30, BioLegend) to detect all leukocytes, CD163 (clone GHI/61; BioLegend) to detect the scavenger receptor for the hemoglobin–haptoglobin complex expressed by macrophages, or isotype-matched irrelevant mouse monoclonal antibodies (BioLegend). Human lung tissue sections were obtained from the National Heart, Lung and Blood Institute-sponsored Lung Tissue Research Consortium (LTRC) (Table S2). Fibroblasts, lung epithelial cells, or lung-tissue sections were prepared and stained with rabbit polyclonal antibodies to Slit2 N-terminal fragment (ab7665; Abcam), as described previously (12). Isotype-matched rabbit anti-chicken IgY antibodies (Bethyl Laboratories) were used as controls. Secondary $F(ab')_2$ biotin-conjugated donkey anti-mouse or donkey anti-rabbit antibodies were from Jackson ImmunoResearch. Lung-tissue sections stained with Slit2 antibodies were analyzed with ImageJ software (61). The percentage area of lung tissue stained with Slit2 antibodies was quantified as a percentage of the total area of the lung tissue, as described previously (23). BAL cytospins and frozen lung-tissue sections (5 μm) were prepared, and immunochemistry was performed as described previously (39). Antibodies to Ly6G (BioLegend) were used to detect neutrophils, CD3 (BioLegend) to detect T cells, CD11b (BioLegend) to detect blood and inflammatory macrophages, CD11c (MBL International) to detect resident lung macrophages and dendritic cells, CD45 (BioLegend) to detect all leukocytes, and CD209b (eBioScience) to detect SIGN-R1–positive dendritic cells. Isotype-matched rat irrelevant antibodies were used as controls. Lung sections were also stained with rabbit antibodies to collagen-I (Abcam), collagen VI (Novus Biologicals), IgY, or sirius red to identify collagen, as described previously (39). To detect fibrocytes, murine lung-tissue sections were stained for CD45 and collagen-I or collagen-VI, as described previously (12, 23). Staining was revealed with DyLight488-conjugated goat anti-rat antibodies (Novus), biotin-conjugated donkey anti-rabbit antibodies (Jackson ImmunoResearch), and streptavidin–Alexa-647 (Invitrogen). Coverslips were mounted with fluorescent mounting medium containing DAPI (Vector Laboratories). Immunofluorescence images were captured on an Olympus FV1000 confocal microscope and analyzed using Olympus Fluoview software.

Statistical Analysis. Statistical analysis was performed using Prism (GraphPad Software). Statistical significance between two groups was determined by t test, or between multiple groups using analysis of variance (ANOVA). Significance was defined as $P < 0.05$.

ACKNOWLEDGMENTS. We thank the staff at Beutel Student Health Services for phlebotomy work. We thank Michael White for isolating human monocytes. We also thank Nehemiah Cox for help with confocal microscopy and critical reading of the manuscript. This work was supported by National Institutes of Health Grant R01 HL118507.

1. Auffray C, Sieweke MH, Geissmann F (2009) Blood monocytes: Development, heterogeneity, and relationship with dendritic cells. *Annu Rev Immunol* 27(1):669–692.
2. Bucala R, Spiegel LA, Chesney J, Hogan M, Cerami A (1994) Circulating fibrocytes define a new leukocyte subpopulation that mediates tissue repair. *Mol Med* 1(1):71–81.
3. Reilkoff RA, Bucala R, Herzog EL (2011) Fibrocytes: Emerging effector cells in chronic inflammation. *Nat Rev Immunol* 11(6):427–435.
4. Bellini A, Mattoli S (2007) The role of the fibrocyte, a bone marrow-derived mesenchymal progenitor, in reactive and reparative fibroses. *Lab Invest* 87(9):858–870.
5. Phillips RJ, et al. (2004) Circulating fibrocytes traffic to the lungs in response to CXCL12 and mediate fibrosis. *J Clin Invest* 114(3):438–446.
6. Haudek SB, et al. (2006) Bone marrow-derived fibroblast precursors mediate ischemic cardiomyopathy in mice. *Proc Natl Acad Sci USA* 103(48):18284–18289.
7. Kisseleva T, et al. (2006) Bone marrow-derived fibrocytes participate in pathogenesis of liver fibrosis. *J Hepatol* 45(3):429–438.
8. Mehrad B, et al. (2007) Circulating peripheral blood fibrocytes in human fibrotic interstitial lung disease. *Biochem Biophys Res Commun* 353(1):104–108.
9. Sakai N, et al. (2010) Fibrocytes are involved in the pathogenesis of human chronic kidney disease. *Hum Pathol* 41(5):672–678.
10. Abe R, Donnelly SC, Peng T, Bucala R, Metz CN (2001) Peripheral blood fibrocytes: Differentiation pathway and migration to wound sites. *J Immunol* 166(12):7556–7562.
11. Pilling D, Buckley CD, Salmon M, Gomer RH (2003) Inhibition of fibrocyte differentiation by serum amyloid P. *J Immunol* 171(10):5537–5546.
12. Pilling D, Fan T, Huang D, Kaul B, Gomer RH (2009) Identification of markers that distinguish monocyte-derived fibrocytes from monocytes, macrophages, and fibroblasts. *PLoS ONE* 4(10):e7475.
13. Hartlapp I, et al. (2001) Fibrocytes induce an angiogenic phenotype in cultured endothelial cells and promote angiogenesis in vivo. *FASEB J* 15(12):2215–2224.
14. Wang JF, et al. (2007) Fibrocytes from burn patients regulate the activities of fibroblasts. *Wound Repair Regen* 15(1):113–121.
15. Cox N, Pilling D, Gomer RH (2014) Serum amyloid P: A systemic regulator of the innate immune response. *J Leukoc Biol* 96(5):739–743.
16. Pilling D, Tucker NM, Gomer RH (2006) Aggregated IgG inhibits the differentiation of human fibrocytes. *J Leukoc Biol* 79(6):1242–1251.
17. Shao DD, Suresh R, Vakil V, Gomer RH, Pilling D (2008) Pivotal Advance: Th-1 cytokines inhibit, and Th-2 cytokines promote fibrocyte differentiation. *J Leukoc Biol* 83(6):1323–1333.
18. Pilling D, Vakil V, Gomer RH (2009) Improved serum-free culture conditions for the differentiation of human and murine fibrocytes. *J Immunol Methods* 351(1-2):62–70.
19. Crawford JR, Pilling D, Gomer RH (2010) Improved serum-free culture conditions for spleen-derived murine fibrocytes. *J Immunol Methods* 363(1):9–20.
20. Maharjan AS, Pilling D, Gomer RH (2010) Toll-like receptor 2 agonists inhibit human fibrocyte differentiation. *Fibrogenesis Tissue Repair* 3(1):23.
21. Curnow SJ, et al. (2010) Distinct types of fibrocyte can differentiate from mononuclear cells in the presence and absence of serum. *PLoS ONE* 5(3):e9730.

22. Balmelli C, Ruggli N, McCullough K, Summerfield A (2005) Fibrocytes are potent stimulators of anti-virus cytotoxic T cells. *J Leukoc Biol* 77(6):923–933.
23. Pilling D, et al. (2007) Reduction of bleomycin-induced pulmonary fibrosis by serum amyloid P. *J Immunol* 179(6):4035–4044.
24. Andersson-Sjöland A, et al. (2008) Fibrocytes are a potential source of lung fibroblasts in idiopathic pulmonary fibrosis. *Int J Biochem Cell Biol* 40(10):2129–2140.
25. Schmidt M, Sun G, Stacey MA, Mori L, Mattoli S (2003) Identification of circulating fibrocytes as precursors of bronchial myofibroblasts in asthma. *J Immunol* 171(1): 380–389.
26. Mori L, Bellini A, Stacey MA, Schmidt M, Mattoli S (2005) Fibrocytes contribute to the myofibroblast population in wounded skin and originate from the bone marrow. *Exp Cell Res* 304(1):81–90.
27. Pilling D, et al. (1999) Interferon-β mediates stromal cell rescue of T cells from apoptosis. *Eur J Immunol* 29(3):1041–1050.
28. Buckley CD, et al. (2001) Fibroblasts regulate the switch from acute resolving to chronic persistent inflammation. *Trends Immunol* 22(4):199–204.
29. McGettrick HM, Butler LM, Buckley CD, Rainger GE, Nash GB (2012) Tissue stroma as a regulator of leukocyte recruitment in inflammation. *J Leukoc Biol* 91(3):385–400.
30. Sorokin L (2010) The impact of the extracellular matrix on inflammation. *Nat Rev Immunol* 10(10):712–723.
31. Cox N, Pilling D, Gomer RH (2014) Distinct Fcγ receptors mediate the effect of serum amyloid p on neutrophil adhesion and fibrocyte differentiation. *J Immunol* 193(4): 1701–1708.
32. Kuhn PH, et al. (2012) Secretome protein enrichment identifies physiological BACE1 protease substrates in neurons. *EMBO J* 31(14):3157–3168.
33. Kang BH, Jensen KJ, Hatch JA, Janes KA (2013) Simultaneous profiling of 194 distinct receptor transcripts in human cells. *Sci Signal* 6(287):rs13.
34. Wang KH, et al. (1999) Biochemical purification of a mammalian slit protein as a positive regulator of sensory axon elongation and branching. *Cell* 96(6):771–784.
35. Guan H, et al. (2003) Neuronal repellent Slit2 inhibits dendritic cell migration and the development of immune responses. *J Immunol* 171(12):6519–6526.
36. Prasad A, Qamri Z, Wu J, Ganju RK (2007) Slit-2/Robo-1 modulates the CXCL12/CXCR4-induced chemotaxis of T cells. *J Leukoc Biol* 82(3):465–476.
37. Tole S, et al. (2009) The axonal repellent, Slit2, inhibits directional migration of circulating neutrophils. *J Leukoc Biol* 86(6):1403–1415.
38. B Moore B, et al. (2013) Animal models of fibrotic lung disease. *Am J Respir Cell Mol Biol* 49(2):167–179.
39. Pilling D, Gomer RH (2014) Persistent lung inflammation and fibrosis in serum amyloid P component (APCs-/-) knockout mice. *PLoS ONE* 9(4):e93730.
40. Chédotal A (2007) Slits and their receptors. *Axon Growth and Guidance,* Advances in Experimental Medicine and Biology, ed Bagnard D (Springer, New York), Vol 621, pp 65–80.
41. Maharjan AS, Roife D, Brazill D, Gomer RH (2013) Serum amyloid P inhibits granulocyte adhesion. *Fibrogenesis Tissue Repair* 6(1):2.
42. Herlihy SE, Pilling D, Maharjan AS, Gomer RH (2013) Dipeptidyl peptidase IV is a human and murine neutrophil chemorepellent. *J Immunol* 190(12):6468–6477.
43. Moore BB, et al. (2005) CCR2-mediated recruitment of fibrocytes to the alveolar space after fibrotic injury. *Am J Pathol* 166(3):675–684.
44. Anselmo MA, et al. (2003) Slit and robo: Expression patterns in lung development. *Gene Expr Patterns* 3(1):13–19.
45. Ye B-Q, Geng ZH, Ma L, Geng J-G (2010) Slit2 regulates attractive eosinophil and repulsive neutrophil chemotaxis through differential srGAP1 expression during lung inflammation. *J Immunol* 185(10):6294–6305.
46. Hohenester E (2008) Structural insight into Slit-Robo signalling. *Biochem Soc Trans* 36(Pt 2):251–256.
47. Dickson BJ, Gilestro GF (2006) Regulation of commissural axon pathfinding by slit and its Robo receptors. *Annu Rev Cell Dev Biol* 22(1):651–675.
48. Geutskens SB, Hordijk PL, van Hennik PB (2010) The chemorepellent Slit3 promotes monocyte migration. *J Immunol* 185(12):7691–7698.
49. Rothberg JM, Hartley DA, Walther Z, Artavanis-Tsakonas S (1988) Slit: An EGF-homologous locus of D. melanogaster involved in the development of the embryonic central nervous system. *Cell* 55(6):1047–1059.
50. Plump AS, et al. (2002) Slit1 and Slit2 cooperate to prevent premature midline crossing of retinal axons in the mouse visual system. *Neuron* 33(2):219–232.
51. Xian J, et al. (2001) Inadequate lung development and bronchial hyperplasia in mice with a targeted deletion in the Dutt1/Robo1 gene. *Proc Natl Acad Sci USA* 98(26): 15062–15066.
52. Wu JY, et al. (2001) The neuronal repellent Slit inhibits leukocyte chemotaxis induced by chemotactic factors. *Nature* 410(6831):948–952.
53. Kanellis J, et al. (2004) Modulation of inflammation by slit protein in vivo in experimental crescentic glomerulonephritis. *Am J Pathol* 165(1):341–352.
54. Chaturvedi S, et al. (2013) Slit2 prevents neutrophil recruitment and renal ischemia-reperfusion injury. *J Am Soc Nephrol* 24(8):1274–1287.
55. Niedermeier M, et al. (2009) CD4+ T cells control the differentiation of Gr1+ monocytes into fibrocytes. *Proc Natl Acad Sci USA* 106(42):17892–17897.
56. Moore BB, et al. (2006) The role of CCL12 in the recruitment of fibrocytes and lung fibrosis. *Am J Respir Cell Mol Biol* 35(2):175–181.
57. White MJV, Glenn M, Gomer RH (2013) Trypsin potentiates human fibrocyte differentiation. *PLoS ONE* 8(8):e70795.
58. National Research Council (2011) *Guide for the Care and Use of Laboratory Animals* (National Academies Press, Washington, DC), 8th Ed.
59. Walters DM, Kleeberger SR (2008) Mouse models of bleomycin-induced pulmonary fibrosis. *Curr Protoc Pharmacol* 40:5.46.1–5.46.17. Unit 5.46.
60. Daubeuf F, Frossard N (2012) Performing bronchoalveolar lavage in the mouse. *Curr Protoc Mouse Biol* 2:167–175.
61. Rasband WS (1997–2014) ImageJ (NIH, Bethesda, MD). Available at imagej.nih.gov/ij/.